Influence of structural heterogeneity of high-strength OCTG tubes on sulfide corrosion cracking resistance.

Artem Davydov[1*], Andrey Zhitenev[1], Natalya Devyaterikova[2], Konstantin Laev[2]

[1]Peter the Great St. Petersburg Polytechnic University, St. Peterburg, Russia
[2]JSC Pervouralsk New Pipe Plant, Pervouralsk, Russia

*E-mail: davydov_ad@spbstu.ru

Keywords: High-strength OCTG, Sulfide corrosion cracking, sulfide stress corrosion tests with low strain rates (SSRT), microstructure, banding, segregation

Abstract.
High-strength OCTG tubes like C110, according to API 5CT (yield strength at least 758 MPa), are subject to requirements in terms of mechanical and corrosion properties. In this work, we studied the influence of seamless tubes microstructure with a 177.8 mm diameter and 10.36 mm wall thickness of class C110 high-strength steel to sulfide stress corrosion cracking (SSC) and sulfide stress corrosion cracking with low strain rates (SSRT). Tubes were obtained from continuous billets by screw piercing with preliminary quenching and tempering. It was established that cracking during the tests always begins from the inner surface of the tube. Rough segregation bands were found on the inner tube surface, which occupies about a third of the thickness. It is shown that the SSRT assessment technique allows to estimate the threshold value of the resistance.

Introduction

During development of deep oil and gas fields, casing is influenced not only by the aggressive environment of the well (H_2S and CO_2), but high pressures and temperatures [1-4]. If low-alloyed steel pipes are exposed to these environments, hydrogen cracking can occur, caused corrosion cracks in the hydrogen sulfide environment (SSC) [5]. Casing of high-strength groups in a corrosion-resistant design used for those conditions, for example C110 according to ANSI/API 5CT (yield strength at least 758 MPa) [6, 7].

Extreme operating conditions require the high quality of the steels and determine the requirements for the level of alloying and purity for detrimental impurities, as well as for the chemical and structural homogeneity of the finished pipes. Therefore, to produce these pipes, it is important to choose the optimal chemical composition of steel and consider that the formation of the final structure is influenced by all redistributions from smelting and casting [8] to rolling [9] and final heat treatment [10].

At satisfactory mechanical properties, determined under static tension, local weak points arise due to non-metallic inclusions and segregations of chemical elements, which can lead to SSC in a corrosive environment (Figure 1, [11]). Near a surface defect (nonmetallic inclusions, solid structural components), pitting may occur [12, 13], hydrogen accumulates, which is then adsorbed, diffuses into the steel, and leads to its embrittlement [11-13]. If segregations and defects are developed into the depth of the pipe, then further opening and development of a corrosion crack occurs along them [11].

Due to the large number of potential causes of steel fracture during tests on SSC, a detailed study of each specific case is required to determine the causes of test failures and to develop technological recommendations to minimize them.
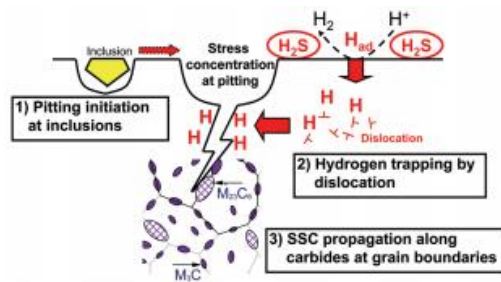
Figure 1. SSC mechanism in high-strength OCTG [9]

In this work, we studied the influence of seamless tubes microstructure with a 177.8 mm diameter and 10.36 mm wall thickness of class C110 high-strength steel 0,3C-Cr-Mn-Mo+0,15(V+Nb+Ti) to sulfide stress corrosion cracking (SSC) and sulfide stress corrosion cracking with low strain rates (SSRT) [14]. Tubes were obtained from continuous billets by screw piercing with preliminary quenching and tempering.

Materials and research methods

Samples were tested for resistance to SSC according to NACE TM0177 [14] and API 5CT [7] requirements for strength group C110 – exposure in 100% hydrogen sulfide for 720 hours at a load of 644 MPa.

As additional studies, the samples were tested at various loads to determine the threshold stress: at 50, 62.5, and 75% of the minimum standard yield strength (MSYS) of 758 MPa. All samples, except those tested at 75% load, showed resistance to SSC (Figure 2).

50%, 720 hours   62,5%, 720 hours   75%, 160 hours   85%, 96 hours   85%, 96 hours

Figure 2. Samples after SSC testing

The study of the corrosion resistance by the SSRT method was carried out using a universal machine UM-10T with an installed reduction gearbox, which allows stretching at speeds from $8.7 \cdot 10^{-8}$ s^{-1} to $8.7 \cdot 10^{-4}$ s^{-1} [14].

Mechanical properties were determined using a universal testing machine UM-10T using standard cylindrical fivefold samples. The macro-hardness of the pipe under study was determined on a transverse template using a TK-2M hardness machine by the Rockwell method.

Longitudinal specimens were cut from the pipe and from the tested samples, which were then ground and polished. Then etching with 4% nitric acid. Metallographic studies were performed using a Reichter light optical microscope equipped with a Thixomet automatic image analyzer. The microhardness of individual structural components was determined using a microhardness tester according to the Vickers method with loads from 1 to 180 g.

The analysis of the dispersed structure and determination of the local chemical composition were studied using a Zeiss Supra scanning electron microscope equipped with an attachment for X-ray spectral analysis.

Results

Mechanical properties

Testing was made on three cylindrical samples taken from different OCTG quadrants in accordance with GOST 1497. The test results are presented in Table 1. It presents the yield strength YS, tensile strength TS, elongation and hardness HRC of the studied samples.

Table 1. Mechanical properties of the OCTG samples.

Sample	YS, MPa	TS, MPa	elongation, %	YS/TS	Hardness, HRC
1	795	878	18.7	0.90	26.0
2	785	875	19.1	0.89	26.5
3	800	880	20.1	0.90	26.0
GOST 31446	758-828	>793	18.0	0.86	<30.0

According to the results of mechanical tests, the material of the OCTG pipe sample corresponds to the strength class C110 (ANSI/API 5CT).

Metallographic analysis

The fracture surface of the samples after testing on SSC at 85% of the yield strength was studied using SEM (Figure 3). Crack nucleation on the samples always occurred from side marked in red, followed by a ductile rupture zone (yellow) and a break zone. The fracture structure in Figure 3a has a brittle fracture. The structure of Figure 3b has numerous ductile fracture pits, which is typical for crack growth zones, the structure of Figure 3c is similar to the previous one, but it has multiple secondary cracks, which corresponds to the break fracture zone.

Fracture surface, ×2000
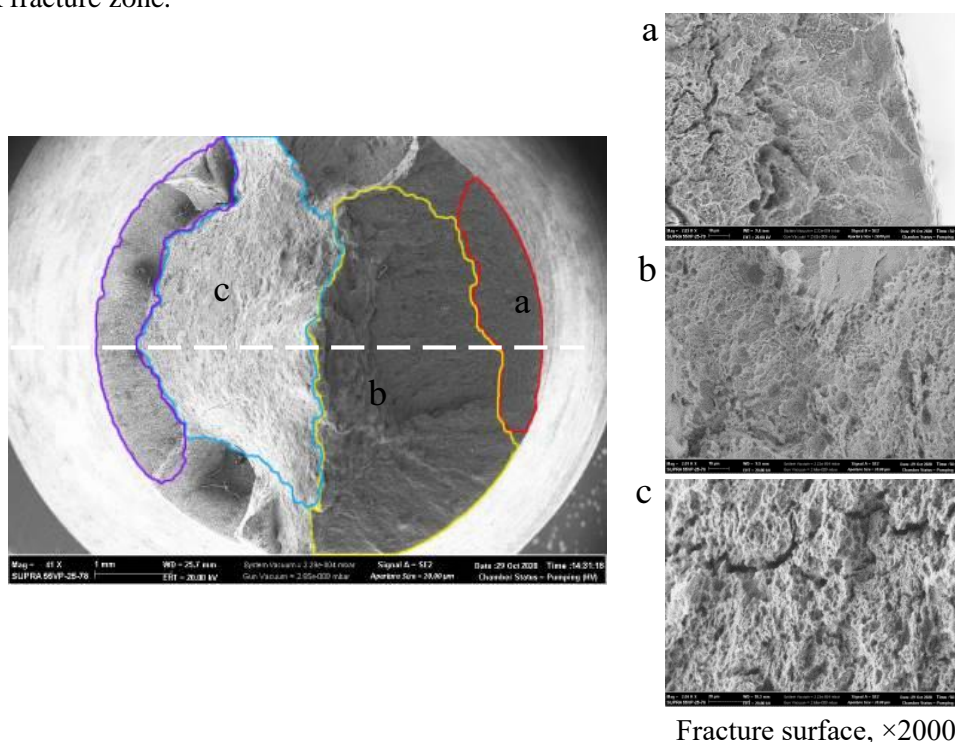
**Figure 3.** Fracture surface of the specimen after testing on SSC 85% YS_{min}

For metallographic studies, longitudinal thin sections (along the dashed line in Figure 3) were cut out from the samples after testing on the SSC so that the fracture surface fell into the thin section. A panoramic view of the structure of the reverse part of the sample is shown in Figure 4.

| Panoramic image, ×50 | Panoramic image, ×200 |
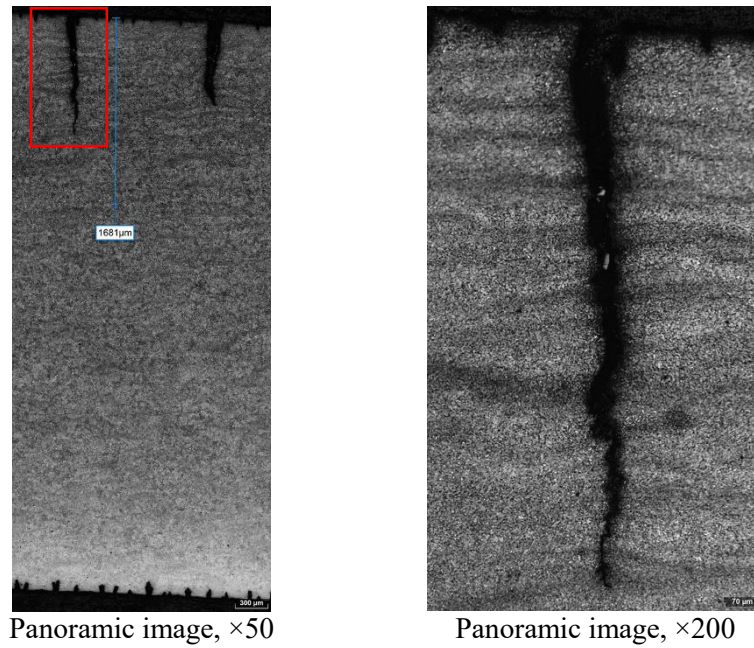
Figure 4. Fracture surface of the specimen after testing on SSC

Dark segregation bands were found on the sample, occupying about a third of the surface on the side of the inner pipe surface. It is from this surface that the destruction of samples always begins during tests on the SSC. Also, the secondary cracks located perpendicular to the axis of the specimen, according to the stress state diagram during testing, as they develop and meet the segregation band, unfold parallel to the specimen axis.

The structure of OCTG samples is composed of tempered martensite and sorbite (Figure 5a). An inhomogeneity was also found along the pipe wall thickness in the form of segregation bands located at the inner surface and occupying about a third of the thickness (Figure 5b).

| Outer surface of OCTG, × 1000 | Inner surface of OCTG, × 1000 |
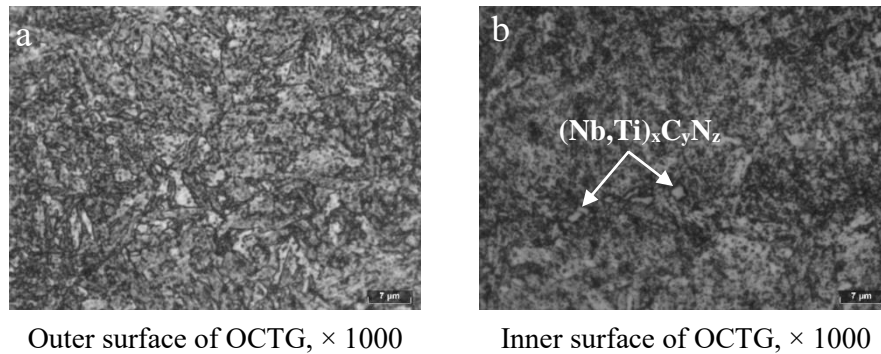
**Figure 5.** OCTG structure at the inner and outer surfaces

This crude structural heterogeneity results in different properties across the pipe, as measured by hardness. Closer to the outer surface of the pipe, the hardness is lower than that of the central part but is within the permissible divergence (about 30 HV). It is important to note that closer to the inner surface, there is an unevenness in hardness caused by the presence of segregation bands. The hardness between the structural inhomogeneities differs by 40 - 50 $HV_{0.18}$, and in the bands, themselves reaches 325 $HV_{0.18}$. Figure 6 shows the structure of the material in dark (left) and bright (right) bands.

×500   ×500

×10000   ×10000

×25000   ×25000
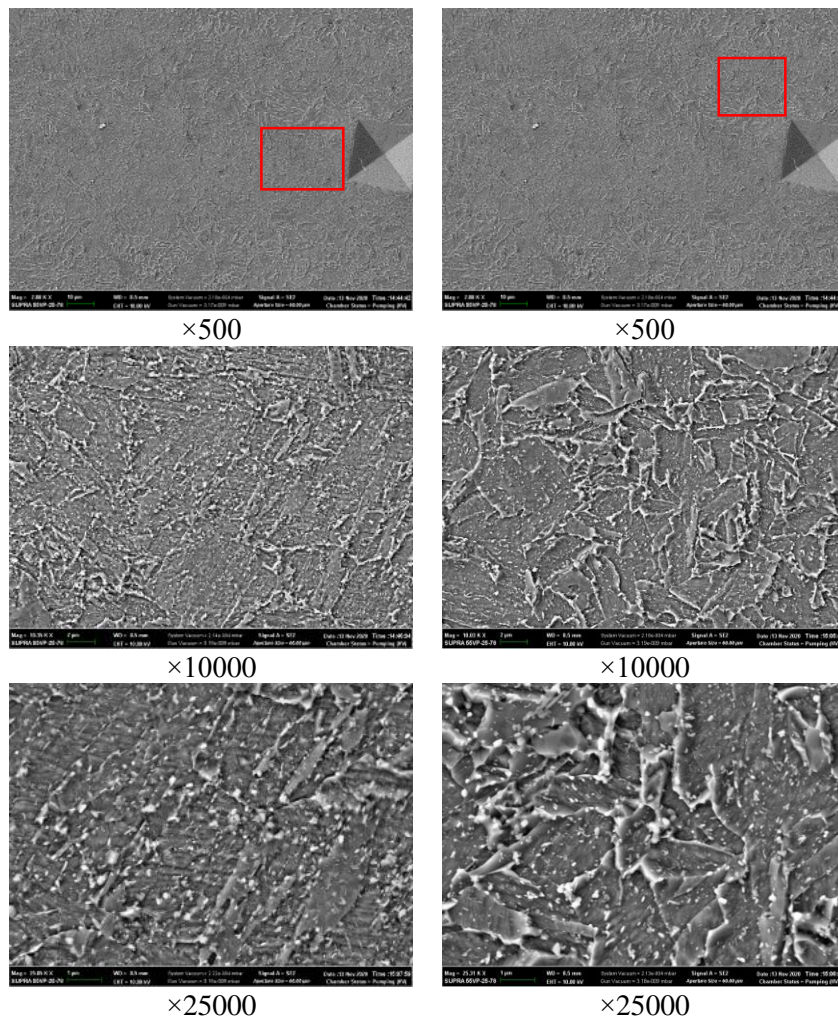
Figure 6. OCTG structure in dark (left) and bright (right) bands

The structure in the segregation bands is more dispersed and contains many small non-metallic inclusions. According to the results of the chemical analysis of the dark and light bands presented in Table 2 and Figure 7, it was determined that in the segregation areas there is an increased content of molybdenum, chromium, and silicon, inherited from the zonal segregations in the central part of the continuous casting.
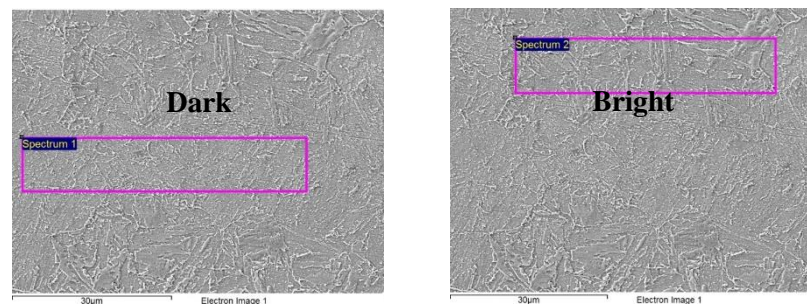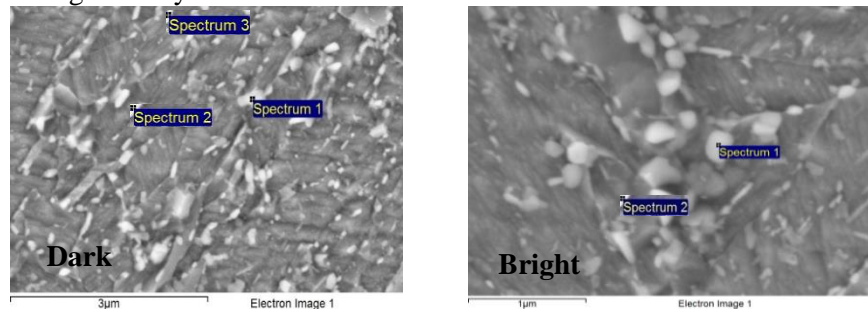

Figure 7. Chemical composition in dark and bright bands

Table 2. Chemical composition, wt. %

Element	Dark band	Bright band
	Spectrum 1	Spectrum 2
Si	0.42	0.32
Cr	1.29	0.96
Mn	0.88	0.93
Fe	95.99	97.07
Mo	1.42	0.71

Figure 8 and Table 3 compares the morphology and composition of carbides in the bright and dark bands. In the bright bands, the carbides are larger, in the dark ones, they are more dispersed. The carbides in dark band have a higher molybdenum content.
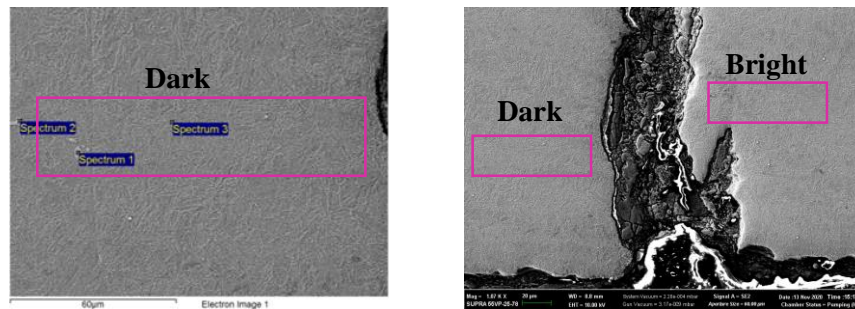

Figure 8. Morphology of carbides in dark and bright bands

Table 3. Carbides composition, wt. %

Element	Dark band			Bright band	
	Spectrum1	Spectrum2	Spectrum3	Spectrum1	Spectrum2
Cr	3.18	3.41	1.55	3.79	6.80
Mn	1.77	1.98	0.96	2.34	4.35
Mo	3.02	2.01	–	2.27	3.23
Fe	92.03	92.14	96.39	91.18	84.24
Ti	–	–	–	–	1.00

Also, crude niobium carbides were found in the dark bands (Table 4 and Figure 9). Judging by their faceted shape (Figure 5b), they were formed at the end of solidification and confirm the liquation nature of the banding found. Similar inclusions are located in the segregation bands in the area of secondary cracks, where the samples failed after SSC. Mostly, these inclusions are niobium carbides, and they are formed during rolling and heat treatment. Coarse niobium and titanium carbonitrides are formed at the end of the solidification of steel.

Figure 9. Nb-Ti Carbides in dark and bright bands

Table 4. Carbides composition, wt.%.

Element	Spectrum1	Spectrum2	Spectrum3
Ti	1.12	1.12	–
Fe	5.76	7.31	95.13
Nb	93.12	91.57	–
Si	–	–	0.45
Cr	–	–	0.91

SSRT testing

SSRT tests were carried out at a tensile speed of 10^{-6} s^{-1}, on standard specimens with a working part of 25.4 mm, diameter 6.35 mm. According to the test results, the samples were cracked at a load of 700, 780, and 790 MPa. Thus, the experimental results do not confirm the tests carried out according to NACE TM 0177 method A, where the breaking stress was less than 644 MPa. The reason for this result may be the uneven localization of segregation bands over the body of the OCTG, which leads a difference

in conditions between the tested samples. Further testing and research is required to investigate these discrepancies and are currently in progress.

Conclusions

The reasons for the initiation of cracks on specimens of high-strength steel (strength group C110) after SSC testing are determined. The main reason for the destruction of samples is the presence of segregation banding (dark and bright bands of different degrees of tempering), localized on one of the sides of the sample, along which destruction occurs. Further investigation of the samples from the pipe showed that the banding is localized at the inner surface of the pipe. The dark bands have increased hardness in comparison with bright ones (320 and 280 HV, respectively), and an increased content of chromium, molybdenum and niobium. In addition to dispersed niobium, molybdenum and chromium carbides formed during rolling and heat treatment, coarse niobium and titanium carbonitrides were found in the bands, which were formed in the solidifying metal due to liquation phenomena. Further testing and research with SSRT method is required to investigate these discrepancies and are currently in progress.

References

[1] Study of corrosion behavior of carbon and low-alloy steels in CO2-containing environments, Kostitsyna, I., Shakhmatov, A., Davydov, A., E3S Web Conf., 121 (2019) 04006, DOI: 10.1051/e3sconf/201912104006

[2] Failure analysis of plunger rod and barrel of sucker rod pumps D. Strekalovskaya, A. Davydov, D. Lyashenko, Tleshev, Maxat 10.24247/ijmperdjun20201414

[3] Natalya Devyaterikova, Marianna Nurmukhametova, Aleksandr Kharlashin, Yegor Popov Types of corrosion damage of tubing in the oilfield E3S Web of Conferences 121, 03001 (2019)

[4] Ermakov B.S, Alhimenko A.A., Shaposhnikov N.O., Tsvetkov A.S., Shirokov A.V., Study of the crystallographic texture of pipe steel // Letters on Materials Volume 10, Issue 1, February 2020, Pages 48-53

[5] Peculiarities of corrosion cracking of high-strength pipe steels in hydrogen sulfide environment A.Alkhimenko, B. Ermakov, E. Alekseeva, S. Mushnikova 10.24247/ijmperdjun20201446

[6] Patent RU 2719618 C1 S. Aleksandrov, K. Laev, I. Shcherbakov, N. Devyaterikova, G. Oshurkov, K. Rogova, A. Pavlov, I. Rodionova Hot-rolled seamless tubing with increased operational reliability for oil-field equipment

[7] ANSI/API Specification 5CT «Specification for Casing and Tubing»

[8] A. G. Shiryaeva, S. G. Chetverikovb, S. G. Chikalova, I. Yu. Pyshmintsevc and P. V. Krylovd Production of Seamless Steel Pipe for Oil and Gas Extractionin Challenging Conditions // Steel in Translation, 2018, Vol. 48, No. 11, pp. 704–711

[9] Tihe Zhou, Peng Zhang, Kate Kuuskman, Erminio Cerilli, Kashif Rehman, Sang-Hyun Cho, Dan Burella Development of Medium-High Carbon Casing/Tubing for Direct Strip Production Complex (DSPC) // Contributed Papers from Materials Science and Technology 2016 (MS&T16)

[10] E. A. Putilova, S. M. Zadvorkin, E. S. Gorkunov, I. N. Veselov, and I. Y. Pyshmintsev (2019) Investigation of structure and properties of low-carbon low-alloyed Cr-Mo pipe steel intended for operating in sour environment // AIP Conference Proceedings 2167, 020291 (2019)

[11] T. Omura, M. Numata, T. Takayama, Y. Arai (2015) Super-high Strength Low Alloy Steel OCTG with Improved Sour Resistance // Nippon Steel & Sumitomo Metal Technical Report No. 107 February 2015. P18-23

[12] Sankara Papavinasam CorrMagnet Consulting Inc., Ottawa, ON, Canada Pitting corrosion 28 // Trends in Oil and Gas Corrosion Research and Technologies

[13] Lekan Taofeek Popoola, Alhaji Shehu Grema, Ganiyu Kayode Latinwo, Babagana Gutti & Adebori Saheed Balogun Corrosion problems during oil and gas production and its mitigation // International Journal of Industrial Chemistry volume 4, Article number: 35 (2013)

[14] A. Alhimenko, A. Kharkov, B. Shemyakinskiy, N. Shaposhnikov Development of the methodology of accelerated testing of oil-gas pipe steels for stress corrosion cracking 2020 Zavodskaya Laboratroiya. Diagnostika Materialov 86(9):70-76

[15] NACE TM 0177 Laboratory Testing of Metals for Resistance to Sulfide Stress Cracking and Stress Corrosion Cracking in H_2S Environments.